Supplementary Figure Legends

Supplementary Figure S1. Gene expression analysis of epidermal marker genes and *TP63*.

A. Screenshot of the UCSC genome browser from normalized RNAPII and RNA-seq ChIP-seq data during keratinocyte differentiation (day 0, 2, 4 and 7 after differentiation initiation) at gene loci of differentiation markers (*KRT14*, *KRT10*, and *LOR*). RNAPII dataset was generated from human primary keratinocytes of one donor (HKC1) and RNA-seq data sets were generated from human primary keratinocytes of two donors (HKC1 and HKC2).

B. Protein immunoblot analysis of epidermal marker genes, *p63*, *KRT14*, *KRT10*, *IVL*, and *LOR* expression during differentiation (day 0, 2, 4 and 7 after differentiation initiation) in HKC1 cells.

C. RT-qPCR analysis of expression of *KRT5, KRT1,* and *IVL* in differentiating keratinocytes from HKC1 and HKC2 at day 0, 2, 4 and 7, using the *hARP* gene as internal control. *KRT5* showed high expression in proliferating and early differentiating cells, *KRT1* shows induced expression in early differentiating cells and is reduced in late differentiated cells, and *IVL* is only detectable at late differentiation stage. (n=1, confirmed by RT-qPCR with biological and technical replicas).

D. Screenshot of the UCSC genome browser from normalized RNAPII and RNA-seq ChIP-seq data at the *TP63* locus during keratinocyte differentiation in HKC1 and HKC2. Expression of exons that are specific for the TA isoform were not detected.

Supplementary Figure S2. Comparison of genome-wide data of RNA-seq, RNAPII ChIP-seq and H3K27ac ChIP-seq.

A. Comparison of RNA-seq gene expression patterns between keratinocyte samples (HKC1 and HKC2) from this study and those of Kretz et al., 2013. The heatmap shows the Spearman rank correlation coefficients between each pair of samples, indicated by both color and number. Columns are in the same order as rows, with the diagonal indicating the correlation of each sample with itself.

B. Heatmap of K-means clustering of RNA-seq expression patterns of differentially expression genes (*P* value < 0.05) from HKC1 (1) and HKC2 (2) at days 0, 2, 4, and 7 of differentiation. Only genes with high expression (*RPKM* > 10) at least at one stage are included. n= number of genes per cluster. Enriched GO terms, HPO terms, and associated disease genes and potential p63 target disease genes per gene cluster are summarized in the table on the right. Complete data are summarized in Supplementary Table S2.

C. Distribution of gene expression levels (log10-transformed RPKM) for RNAPII ChIP-seq and RNA-seq data of HKC1. Data for all days are combined.

D. Heatmap of PAM clustering (clusters 1-6, top to bottom) of per-gene rank differences between RNAPII ChIP-seq and RNA-seq expression levels of HKC1. Genes were ranked according to their RNA expression or RNAPII occupancy, and the difference in their RNA vs RNAPII rank is shown for each day. Y-axis: genes, X-axis: days. Colors indicate RNA-seq minus RNAPII rank difference, ranging from orange (RNA expression rank > RNAPII occupancy rank) to purple (RNAPII occupancy rank > RNA expression rank). Clusters are indicated in the color bar on the left, colored according to the degree of non-coding RNA enrichment (red) or

depletion (blue). The cluster at the bottom (red) showed higher expression detected by RNAPII ChIP-seq, and this cluster is enriched for non-coding RNAs. Complete data are summarized in Supplementary Table S3.

E. Spearman correlation analysis of genome-wide RNA-seq, RNAPII-, and H3K27ac ChIP-seq signals (RPKM per gene) at the gene body during epidermal differentiation of HKC1.

Supplementary Figure S3. Transcribed miRNAs in keratinocytes.

A. Heatmap of all identified transcribed miRNAs outside gene body regions determined by RNAPII occupancy at the pri-miRNA region at four stages of HKC1 keratinocyte differentiation.

B. Screenshot from genome browser (UCSC) of normalized RNA-seq (shades of blue), RNAPII ChIP-seq (shades of green), H3K27ac ChIP-seq (shades of purple), and p63 ChIP-seq (shades of red) signals at *miRNA-203* and *miRNA-205* during HKC1 keratinocyte differentiation.

Supplementary Figure S4. Genomic distribution of p63 binding sites relative to RefSeq genes.

A. Peak detection analysis of p63 ChIP-seq data with a stringent statistical threshold (*P* value of 10^{-9}) of HKC1 resulted in the identification of 32,888, 31,995, 29,539, and 28,169 p63 binding sites at differentiating day 0, 2, 4, and 7, respectively. The total of p63 binding sites identified in all datasets was 38,890. Genomic distribution of p63-binding site (p63BS) location of these 38,980 peaks relative to RefSeq genes was determined at promoters (5kb

upstream of TSS, first exon and first intron), in intragenic regions (all introns and exons except first), <25 kb (5-25 kb upstream or 25 kb downstream of last exon), and intergenic regions (everything else). The asterisk represents significant enrichment.

B. Bandplot of p63 occupancy at all p63 binding sites (genomic regions of a 4kb window with summits of p63 binding sites in the middle in each panel) during HKC1 keratinocyte differentiation. The average p63 signal is depicted in black. p63 binding signal range of 50% and 90% of p63 binding sites is depicted in purple and light purple, respectively.

Supplementary Figure S5. Screenshots of genome browser of RNA-seq, RNAPII ChIP-seq, H3K27ac ChIP-seq and p63 ChIP-seq data at *RUNX1*, *CDH3*, *LCE1B/LCE1C*, *Involucrin*, *KRT1,* and *PRDM1* loci from four stages of keratinocyte differentiation of HKC1.

A. Screenshot of the UCSC genome browser at the genomic locus surrounding *GRASP* and *PRRX*. H3K27me3 track generated from NHEK cells are depicted in pink.

B. Screenshot of the UCSC genome browser at the genomic locus surrounding *RUNX1*.

C. Screenshot of the UCSC genome browser at the genomic loci surrounding *CDH3, LCE1B/LCE1C*, and *Involucrin (IVL)*.

D. Screenshot of the UCSC genome browser at the genomic loci surrounding *KRT1* and *PRDM1* with clustered epidermal enhancer marked with a black box.

Normalized RNA-seq, in decreasing shades of blue during differentiation; RNAPII ChIP-seq, in decreasing shades of green; H3K27ac ChIP-seq, in decreasing shades of purple; and p63 ChIP-seq, in decreasing shades of red. Detected individual p63 binding sites and cl-p63BS are marked with a black box.

List of Supplementary tables:

Supplementary Table S1: Nine clusters of genes with distinct expression patterns based on K-means clustering of genes identified in RNAPII ChIP-seq (RPKM .1.0)

1A: Gene clustering and RPKM of RNAPII ChIP-seq results

1B: Gene Ontology of gene clusters from RNAPII ChIP-seq

1C: HPO analysis of gene clusters from RNAPII ChIP-seq

1D: p63BS association to nearest genes identified in RNAPII ChIP-seq

Supplementary Table S2: Six clusters of genes with distinct expression patterns based on K-means clustering of genes identified in RNA-seq (P value < 0.05, cuffdiff2 software, and with an RPKM >10)

2A: Gene clustering and RPKM of RNA-sequencing results

2B: Gene Ontology of gene clusters from RNA-seq

2C: HPO analysis of gene clusters from RNA-seq

2D: p63BS association to nearest genes identified in RNA-seq

Supplementary Table S3: Comparison of RNAPII ChIP-seq and RNA-seq analysis

3A: Rank difference of RNA-seq gene rank - RNAPII ChIP-seq gene rank

3B: GO annotation of genes from different clusters with ranking differences between RNA ChIP-seq and RNA-seq

3C: non-coding RNA enrichment/depletion log2 fold changes per-cluster with rank differences RNAPII ChIP-seq versus RNA-seq

3D: *P*-values for tendency of non-coding RNAs to have higher RNAPII occupancy rank than RNA-seq expression rank (HKC1)

Supplementary Table S4: microRNAs identified by RNAPII ChIP-seq

4A: Identified pri-miRNAs using RNAPII ChIP-seq data

4B: Identified pri-miRNAs with p63BS and information on their H3K27ac status

4C: Spearman correlation of pri-miRNAs from RNAPII ChIP-seq signal versus RNA-seq signal

Supplementary Table S5: p63 binding sites identified during epidermal differentiation

5A: P63 binding sites identified in HKC1 at day0 using MACS2

5B: P63 binding sites identified in HKC1 at day2 using MACS2

5A: P63 binding sites identified in HKC1 at day4 using MACS2

5A: P63 binding sites identified in HKC1 at day7 using MACS2

5E: All 38,980 identified p63 binding sites (p63BS)

Supplementary Table S6: Co-localization of p63 binding sites and H3K27ac mark during epidermal differentiation

6A: p63BS that overlap H3K27ac marker from ENCODE NHEK cells

6B: H3K27ac peaks identified in HKC1 at day0 using MACS2

6C: H3K27ac peaks identified in HKC1 at day2 using MACS2

6D: H3K27ac peaks identified in HKC1 at day4 using MACS2

6E: H3K27ac peaks identified in HKC1 at day7 using MACS2

6F: p63BS that overlap H3K27ac occupancy identified at four stages of keratinocyte differentiation

6G: p63BS that overlap H3K27ac and nearby genes

Supplementary Table S7: Motif enrichment at identified active and inactive p63BS

Supplementary Table S8: Co-activator RUNX1 and TFAP2A binding to p63 binding sites

8A: RUNX1 motif location in active p63BS

8B: RUNX1 ChIP-qPCR results

8C: TFAP2 ChIP-qPCR results

Supplementary Table S9: p63 binding sites clusters based on H3K27ac dynamics and associated motifs

9A: Clusters of active p63BS with dynamic H3K27ac occupancy

9B: Clusters of active p63BS with dynamic H3K27ac occupancy to nearby gene with associated RNAPII gene cluster information

9C: Motif enrichment at clusters of active p63BS with dynamically identified H3K27ac occupancy

Supplementary Table S10: p63BS enrichment near transcribed genes (detected by RNAPII ChIP-seq)

Supplementary Table S11: clustered epidermal enhancers

11A: Identified clustered epidermal enhancers

11B: Identified genes near clustered epidermal enhancers

11C: GO analysis of genes near clustered epidermal enhancers

11D: HPO analysis of genes near clustered epidermal enhancers

Supplementary Table S12: potential p63 target genes with p63 binding sites

12A: Genes identified near all 38,980 p63BS

12B: GO annotation of genes near all 38,980 p63BS

Supplementary Table S13: previously reported epidermal disease genes and p63-regulated genes

13A: Gene list of genes with a known role in epidermal diseases and information from RNAPII ChIP-seq and RNA-seq

13B: Gene list of genes with a known role in epidermal diseases and information on their closest p63BS

13C: Gene list of genes with identified by p63 knock-down or knockout in previously described studies.

13D: Gene list of genes identified by p63 knock-down or knockout in previously described studies with p63BS information

Supplementary Table S14: clustered p63 binding sites (cl-p63BS)

14A: clustered p63 binding sites (cl-p63BS)

14B: Nearby genes of cl-p63BS

14C: GO analysis of genes near cl-p63BS

14D: HPO association analysis of genes near cl-p63BS

Supplementary Table S15: cl-p63BS that overlap clustered epidermal enhancers

15A: cl-p63BS that overlap clustered epidermal enhancers

15B: Genes nearby clustered epidermal enhancers which overlap cl-p63BS

15C: GO analysis of genes nearby clustered epidermal enhancers which overlap cl-p63BS

15D: HPO analysis of genes nearby clustered epidermal enhancers which overlap cl-p63BS

Supplementary Table S16: Clustered epidermal enhancers that do not overlap cl-p63BS

16A: Clustered epidermal enhancers that do not overlap cl-p63BS

16B: Genes identified near clustered epidermal enhancers that do not overlap cl-p63BS

16C: GO analysis of genes near clustered epidermal enhancers that do not overlap cl-p63BS

16D: HPO analysis of genes near clustered epidermal enhancers that do not overlap cl-p63BS

Supplementary Table S17: cl-p63BS that do not overlap clustered epidermal enhancers

17A: cl-p63BS that do not overlap clustered epidermal enhancers

17B: Genes identified near cl-p63BS that do not overlap clustered epidermal enhancers

17C: GO analysis of genes near cl-p63BS that do not overlap clustered epidermal enhancers

17D: HPO analysis of genes near cl-p63BS that do not overlap clustered epidermal enhancers

Supplementary Table S18: RT q-PCR primers

Supplementary Table S19: Statistics of sequencing.

Supplementary Table S20: summary of average z-scores used in Figure 1C.

20A: Overview of average z-scores and standard deviations per stage for genes identified in both RNAPII ChIP-seq and RNA-seq for each genecluster identified using RNAPII ChIP-seq

20B: z-scores for genes identified in both RNAPII ChIP-seq and RNA-seq for gene cluster 1 identified by RNAPII ChIP-seq

20C: z-scores for genes identified in both RNAPII ChIP-seq and RNA-seq for gene cluster 2 identified by RNAPII ChIP-seq

20D: z-scores for genes identified in both RNAPII ChIP-seq and RNA-seq for gene cluster 3 identified by RNAPII ChIP-seq

20E: z-scores for genes identified in both RNAPII ChIP-seq and RNA-seq for gene cluster 4 identified by RNAPII ChIP-seq

20F: z-scores for genes identified in both RNAPII ChIP-seq and RNA-seq for gene cluster 5 identified by RNAPII ChIP-seq

20G: z-scores for genes identified in both RNAPII ChIP-seq and RNA-seq for gene cluster 6 identified by RNAPII ChIP-seq

20H: z-scores for genes identified in both RNAPII ChIP-seq and RNA-seq for gene cluster 7 identified by RNAPII ChIP-seq

20I: z-scores for genes identified in both RNAPII ChIP-seq and RNA-seq for gene cluster 8 identified by RNAPII ChIP-seq

20J: z-scores for genes identified in both RNAPII ChIP-seq and RNA-seq for gene cluster 9

identified by RNAPII ChIP-seq

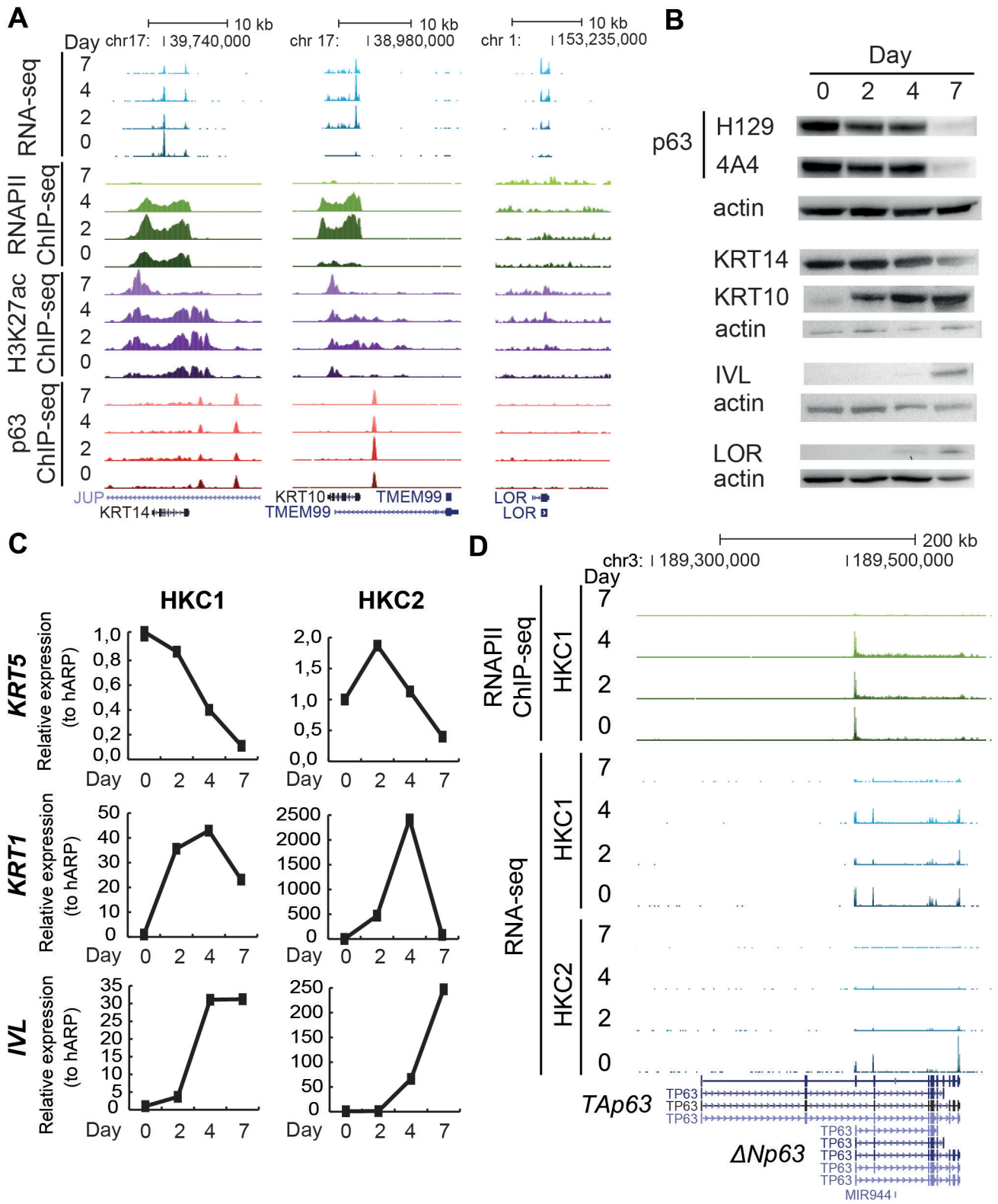
A
Day
chr17: 39,740,000
chr 17: 38,980,000
chr 1: 153,235,000
10 kb
RNA-seq
RNAPII ChIP-seq
H3K27ac ChIP-seq
p63 ChIP-seq
JUP
KRT14
KRT10
TMEM99
LOR
B
Day
0 2 4 7
p63
H129
4A4
actin
KRT14
KRT10
actin
IVL
actin
LOR
actin
C
HKC1
HKC2
KRT5
KRT1
IVL
Relative expression (to hARP)
Day 0 2 4 7
D
chr3: 189,300,000
189,500,000
200 kb
RNAPII ChIP-seq
RNA-seq
HKC1
HKC2
TAp63
ΔNp63
TP63
MIR944

Fig. S1

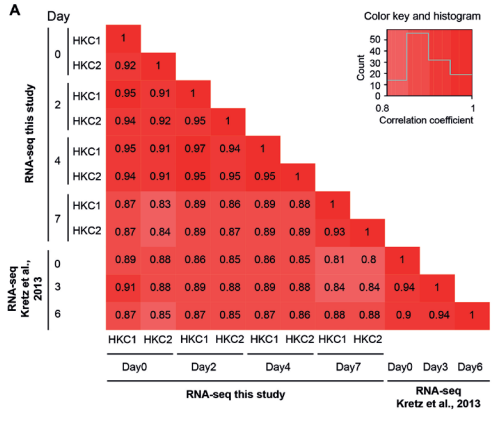

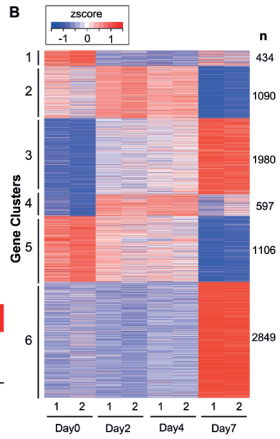

Gene Cluster	GO terms	HPO analysis	Disease genes	Disease genes with active p63BS
1	Nucleosome organization Chromatin assembly or disassembly Protein complex assembly Cell adhesion	Blistering	*ITGB4* *HRAS*	*ITGB4*
2	Oxidation reduction Cell redox homeostasis Cellular protein localization	Dermatological manifestations of systemic disorders		
3	Epidermal cell differentiation Ectoderm development Keratinization Proteolysis localization Regulation of cell death	Dry skin Thickened skin	*LOR* *ABCA12* *SLURP1* *FLG* *TGM1* *CLDN1* *SPINK5* *GJB4* *CYP4F22* *NIPAL4* *ALOX12B* *PTPN11* *ABHD5*	*ALOX12B* *CLDN1* *NIPAL4* *GJB4* *FLG* *ABCA12* *PTPN11* *CYP4F22* *ABHD5*
4	Oxidation reduction Apoptosis Epidermis development Ectoderm development Heterophilic cell adhesion	Hyperkeratosis	*KRT2* *GJB6* *DSG1* *CSTA* *KRT1* *KRT10*	*KRT10* *GJB6* *DSG1* *CSTA* *KRT1*
5	Nucleosome assembly DNA packaging Mitosis Cell cycle process	Pigmentation abnormalities	*AP1S1* *CDH3* *TP63* *COL17A1*	*COL17A1* *TP63* *CDH3*
6	Keratinization Epidermal cell differentiation Positive regulation of gene expression	Vascular defects Eyebrow malformations	*CDSN* *ATP2A2* *STS* *BRAF*	*ATP2A2* *BRAF*

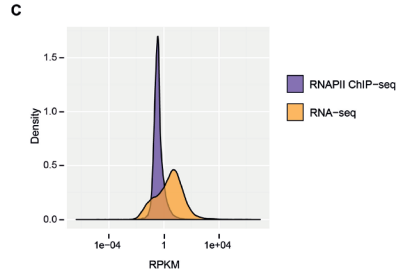

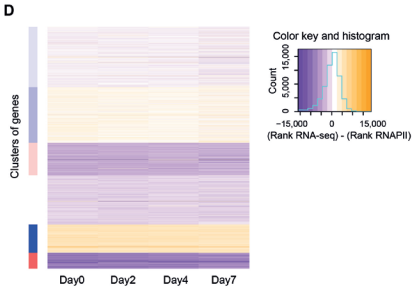

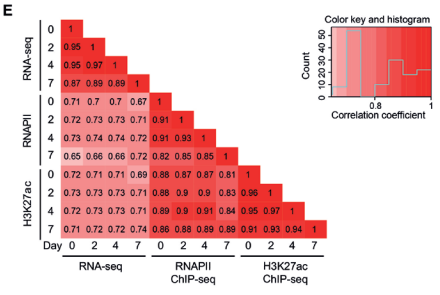

Fig. S2

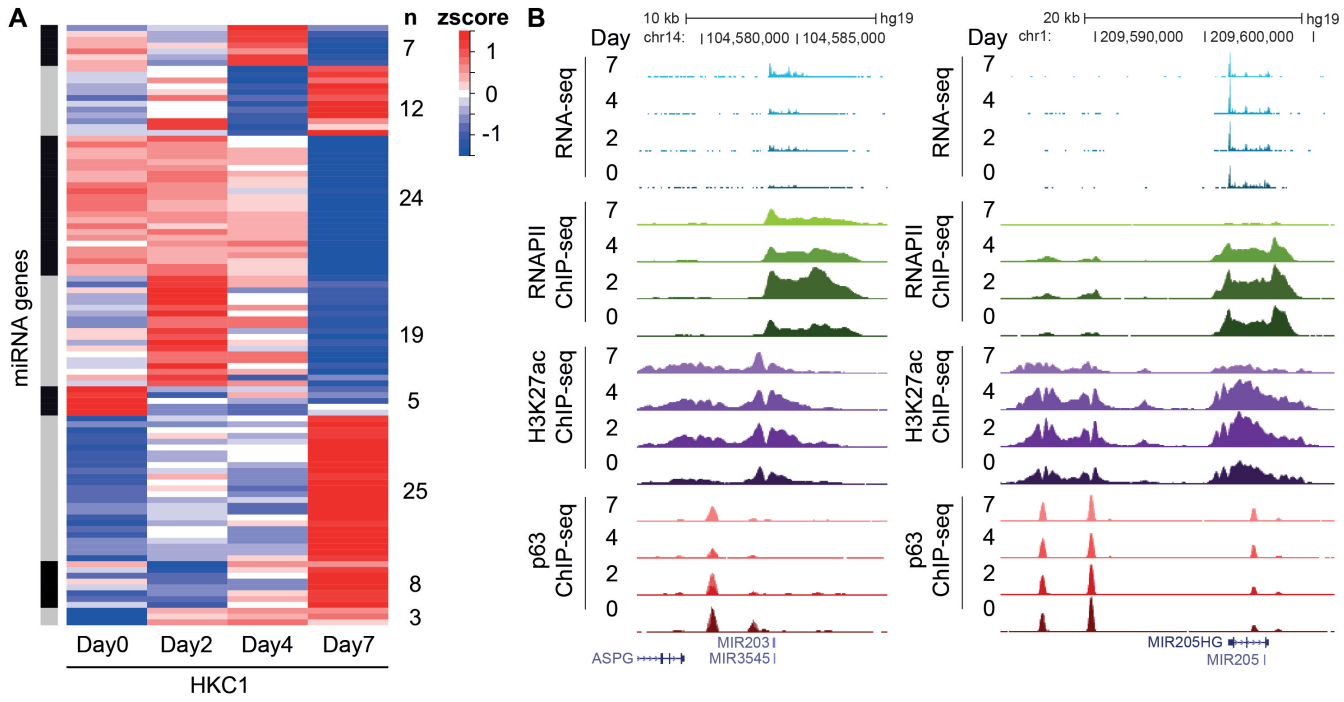
A
n
zscore
1
0
-1
7
12
24
19
5
25
8
3
miRNA genes
Day0
Day2
Day4
Day7
HKC1
B
10 kb
hg19
Day
chr14:
104,580,000
104,585,000
RNA-seq
RNAPII ChIP-seq
H3K27ac ChIP-seq
p63 ChIP-seq
ASPG
MIR203
MIR3545
20 kb
hg19
Day
chr1:
209,590,000
209,600,000
MIR205HG
MIR205

Fig. S3

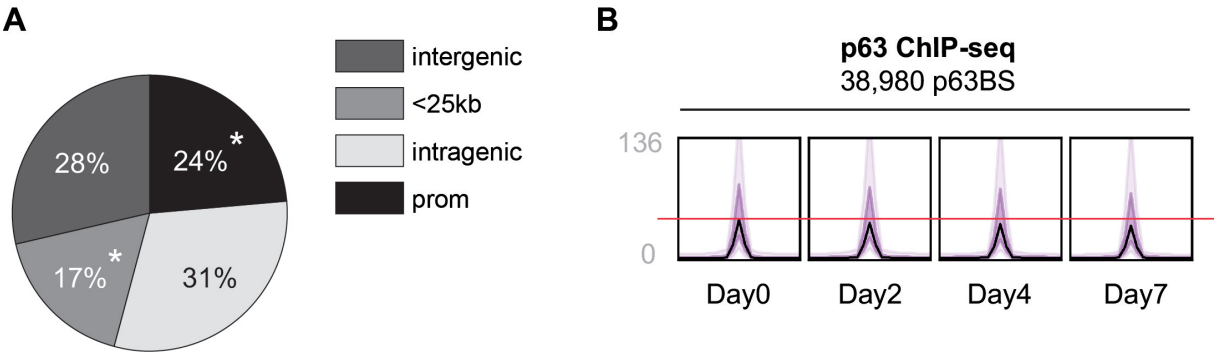
A
28%
24%*
17%*
31%
intergenic
<25kb
intragenic
prom
B
p63 ChIP-seq
38,980 p63BS
136
0
Day0
Day2
Day4
Day7

Fig. S4

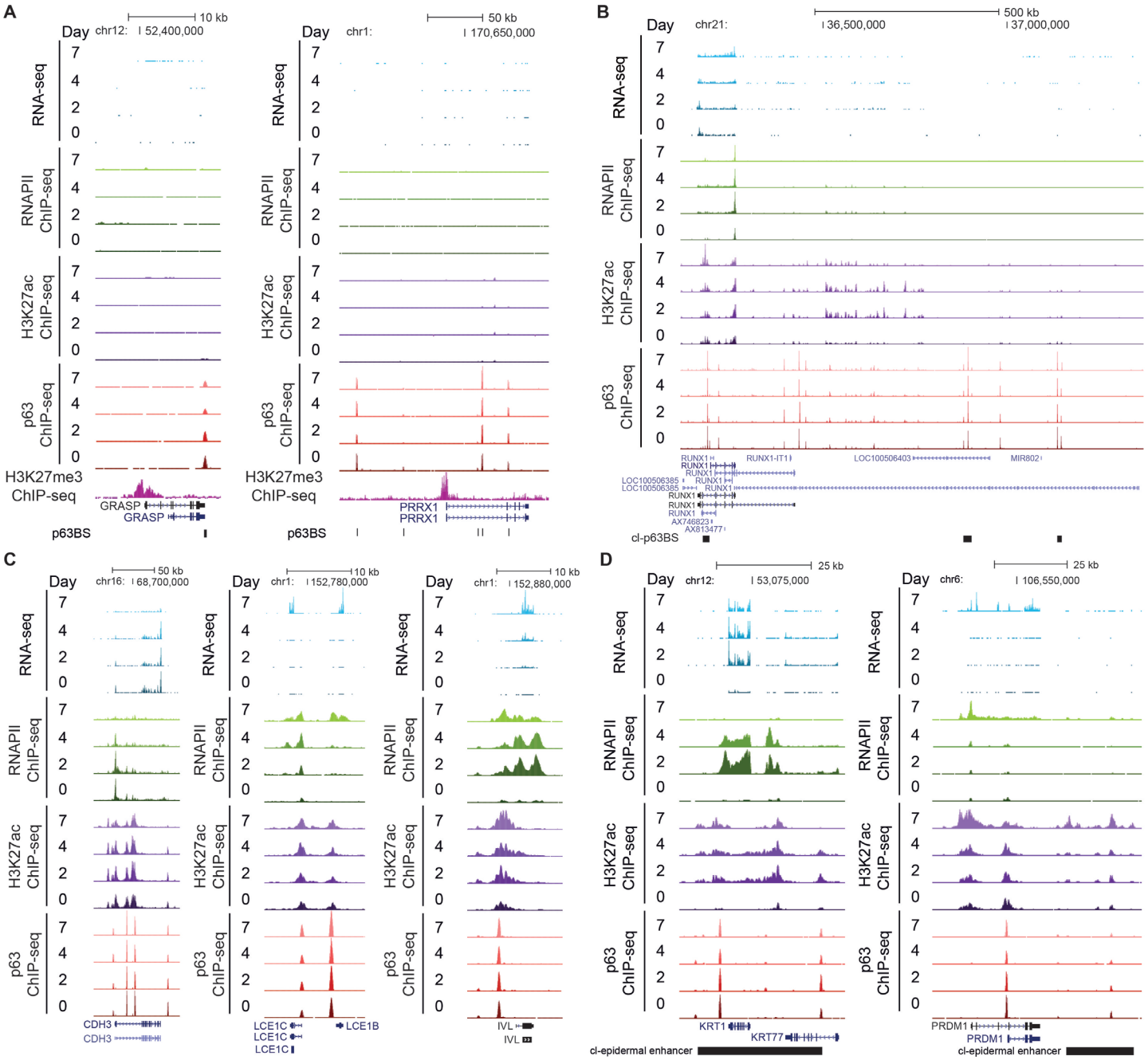
A
Day
chr12: 52,400,000
10 kb
RNA-seq
RNAPII ChIP-seq
H3K27ac ChIP-seq
p63 ChIP-seq
H3K27me3 ChIP-seq
GRASP
p63BS
chr1: 170,650,000
50 kb
PRRX1
B
chr21:
36,500,000
37,000,000
500 kb
RUNX1
RUNX1-IT1
LOC100506403
MIR802
cl-p63BS
C
chr16: 68,700,000
50 kb
CDH3
chr1: 152,780,000
10 kb
LCE1C
LCE1B
chr1: 152,880,000
IVL
D
chr12: 53,075,000
25 kb
KRT1
KRT77
cl-epidermal enhancer
chr6: 106,550,000
PRDM1

Fig. S5